MONITORING AND MITIGATION OF CLOSE PROXIMITIES IN LOW EARTH ORBIT

S. Aida[(1)], T. Patzelt[(2)], L. Leushacke[(2)], M. Kirschner[(1)], R. Kiehling[(1)]

[(1)]Deutsches Zentrum für Luft- und Raumfahrt (DLR), German Space Operations Center (GSOC), 82234 Wessling, Germany, +49(0)8153-28-2158, saika.aida@dlr.de
[(2)]Research Establishment for Applied Science (FGAN), Research Institute for High Frequency Physics and Radar Techniques (FHR), Neuenahrer Str. 20, 53343 Wachtberg, Germany, +49(0)228-9435-200, leushacke@fgan.de, patzelt@fgan.de

ABSTRACT

The German Space Operations Center (GSOC) is currently building up an operational proximity monitoring and mitigation system. Proximity events are detected based on the "Two-line Elements" (TLEs) from the US Strategic Command (USSTRATCOM) and precise orbit information from locally operated missions.

Despite evident deficiencies in the quality and timeliness of the available orbit information, TLEs are currently the only source of orbit information for the numerous space objects. While an overly trust in the quality of the orbital data might result in an underestimation of the true collision risk, a pessimistic accuracy assessment would result in frequent proximity warnings. The TLE uncertainty needs to be carefully assessed to avoid such implications. Even after a realistic error analysis, the orbit information of a possible jeopardising object has to be refined for a proper planning and implementation of collision avoidance manoeuvres. For this purpose, the use of FGAN radar tracking is currently planned, for which an accuracy assessment is to be considered.

In this paper, the proximity statistics and TLE accuracy analysis as well as the FGAN tracking campaign are discussed, together with their application to the collision risk management of satellites in a Low-Earth-Orbit (LEO). The cumulative frequency of predicted proximities is first estimated for the selected GSOC missions based on a one-year simulation. The TLE accuracy is then discussed by comparing ephemerides derived from TLEs with those derived from precise orbit determination of locally controlled satellites. As a special case, the recent collision between a Cosmos and an Iridium satellite is also analysed. Complementary to these assessments, the orbit prediction accuracy using FGAN tracking is discussed from campaign results. The paper concludes with a discussion of the operational application to the active proximity monitoring and mitigation strategies.

1. INTRODUCTION

The ever increasing population of objects in the near Earth environment has created growing concerns among satellite owners and control centres about the safety of their missions. The GSOC has started to build-up an operational proximity monitoring and mitigation system in cooperation with the FGAN-FHR Research Institute for High Frequency Physics and Radar Techniques.

Contrary to locally operated satellites, high accurate orbital parameters are not available for the bulk of other space objects. Currently, the TLE catalogue maintained by the USSTRATCOM constitutes the only publicly available and reasonably comprehensive orbit information. Despite evident deficiencies in the quality and timeliness of the available orbit information, it is currently a mandatory element of any operational proximity monitoring. The careful assessment of the TLE

accuracy is therefore required to reveal the inherent modelling accuracy of the SGP4 analytical orbit model, as well as the orbit determination and orbit prediction accuracy for TLEs provided by USSTRATCOM.

Even after a realistic error analysis, the exclusive use of TLE data is insufficient for a proper planning and implementation of collision avoidance manoeuvres. The orbit information of a possible jeopardising object has to be refined in due time before a predicted proximity if a predefined threshold of collision probability or safety distance is violated. To this end, the use of FGAN's unique Tracking and Imaging Radar (TIRA) in Wachtberg, Germany, is foreseen. The orbit refinement using FGAN tracking is necessary for a consolidated decision and implementation of an evasive manoeuvre.

For the operational management of the collision risk for LEO satellites, the proximity statistics and TLE accuracy analysis as well as the improvement of the orbit information by a FGAN tracking campaign are assessed in the paper. The cumulative frequency of predicted proximities is first estimated for the selected GSOC missions based on a one-year simulation. The TLE accuracy is then discussed in two parts. First, the special case of the recent collision between Cosmos 2251 and Iridium 33 is analysed. The second analysis is done by comparing TLE orbit data with accurate orbit information from locally controlled space missions. Complementary to these assessments, the radar based orbit determination is discussed in more detail and sample campaign results are presented. The paper concludes with a discussion of the operational implications of active proximity monitoring and mitigation strategies.

2. ONE-YEAR PROXIMITY ANALYSIS OF TERRASAR-X AND GRACE-1 AGAINST TLE CATALOGUED OBJECTS

To estimate the encounter risk for the satellites operated by GSOC, statistical frequency of predicted proximities was analysed. This proximity analysis was performed for two selected GSOC ongoing missions in LEO, GRACE-1 and TerraSAR-X (GRA/TSX), against all objects in the bulk of the TLE catalogue. Orbit parameters (height *h*, inclination *i*, eccentricity *e*) of these satellites are shown in Table 1.

GSOC has developed a collision risk assessment software which detects proximity events and estimates the associated collision risk. Using this tool, one-year proximity events between GRA/TSX and all objects in the TLE catalogue of a specific date were simulated. Ephemerides of GRA/TSX at the epoch of February 17th, 2009 and TLEs in a catalogue (containing 12939 objects) which was provided by USSTRATCOM on the same day were used as the initial state, and propagated up to a year later. The cumulative frequency of predicted proximities was evaluated as a function of the minimum distance and its radial component. The radial component shows the possible closest distance of two satellites' orbital arcs, since the closest approach occurs in the vicinity of the orbital node. Considering the large position error in the along-track direction, which is discussed in the following sections, it would be safe to estimate the proximity risk with the radial distance. Although a realistic prediction over such long period is not exactly possible, proximity statistics can be obtained in such a way.

Table 1 Orbit Parameters of GRACE-1 and TerraSAR-X

	h [km]	*i* [deg]	*e*
GRACE-1	450	89.0	0.0013
TerraSAR-X	514	97.4	0.0012

The number of detected close approaches with a minimum distance smaller than 10.0 km is shown in Table 2. The proximity frequencies for GRACE-1 and TerraSAR-X show similar results. For example, a close approach of < 5.0 km is expected ca. 100 times in a year for both satellites. Proximity events were also categorised by the distance of radial separation. At the distance of < 5.0 km, proximity events in radial separation are twice as frequent as those in minimum distance, which is almost the same to both satellites.

Table 2 Frequency of close approaches during one year

GR1	Distance [km]	< 0.5	< 1.0	< 1.5	< 2.0	< 2.5	< 5.0	< 10.0
	Min.dist	1	4	9	16	22	96	319
	Radial	21	46	72	91	107	206	319
TSX	Distance [km]	< 0.5	< 1.0	< 1.5	< 2.0	< 2.5	< 5.0	< 10.0
	Min.dist	0	2	8	12	29	117	424
	Radial	27	52	73	94	124	251	424

3. COLLISION EVENT ANALYSIS OF IRIDIUM/COSMOS

In this section, the TLE accuracy is discussed using the special case of the recent collision between Cosmos 2251 and Iridium 33, which occurred on February 10th in 2009, at 16:56 UTC (at an altitude of 788.6 km). TLEs of the satellites shortly before the collision and TLEs of the corresponding debris shortly after the collision were analysed by propagating forwards and backwards up to the estimated collision epoch.

3.1 Collision prediction accuracy using TLEs

TLE sets of Cosmos and Iridium up to 7 days before the time of the closest approach (TCA) were extracted, and the collision event was reconstructed for each TLE set. For all cases, the closest approach was detected near the epoch of the estimated collision time. Table 3 shows the detected closest approach for all 14 TLE sets. In general, the minimum distance decreases for TLEs close to the TCA epoch. Nevertheless, the latest TLE set (~1 day before TCA) predicts a minimum distance of around 600 m. On the other hand, the values for radial separation indicate the criticality of the conjunction.

Table 3 Collision prediction of COSMOS and IRIDIUM

TCA	TCA since TLE epoch [days]		Min.dist	Radial
[UTC]	COSMOS	IRIDIUM	[km]	[km]
16:55:59.670	7.29	7.06	1.752	0.172
16:55:59.742	6.24	6.36	1.812	0.141
16:55:59.928	5.75	5.32	0.117	0.113
16:55:59.916	4.77	3.92	1.243	0.078
16:55:59.893	3.58	3.22	0.688	0.102
16:55:59.770	2.26	2.31	0.984	0.045
16:55:59.806	1.21	1.34	0.584	0.041

3.2 Comparison with TCA position using forward and backward propagation

For further prediction error assessment, the same 14 TLEs were propagated to the TCA, and compared with the satellite position at the time derived from the latest TLE set before TCA (see the bottom line of Table 3) as reference.

Results are shown in Table 4. Differences in the radial (R) and cross-track direction (N) are relatively small and below 100 m for all the TLEs. On the other hand, in the along-track direction (T) the difference becomes nearly 2 km at a maximum and its evolution shows a random behaviour.

Table 4 Comparison of propagated COSMOS and IRIDIUM TLEs with predicted TCA position

COSMOS TLE	Difference from COSMOS $_{TCA}$			IRDIUM TLE	Difference from IDIRIUM $_{TCA}$		
TCA since TLE epoch [days]	R [km]	T [km]	N [km]	TCA since TLE epoch [days]	R [km]	T [km]	N [km]
7.29	-0.099	0.097	0.077	7.06	0.031	2.016	-0.024
6.24	-0.078	-0.480	0.049	6.36	0.021	1.503	-0.026
5.75	-0.066	-0.412	0.058	5.32	0.007	-1.347	-0.022
4.77	-0.051	-1.349	0.031	3.92	-0.013	-0.262	-0.002
3.58	-0.041	-0.750	0.086	3.22	0.021	-0.476	0.008
2.26	-0.014	-0.064	0.044	2.31	-0.010	0.637	0.006
1.21	0.000	0.000	0.000	1.34	0.000	0.000	0.000

Besides TLEs of the satellites before the collision, TLEs of the created debris parts can also be used to estimate TLE accuracies since they emerged from a single orbital position. TLEs of 22 debris parts (15 from Cosmos, and 7 from Iridium) were first provided by USSTRATCOM 6 days after the collision. 15 objects from Cosmos were selected among them, and their TLEs were compared with the last Cosmos position (at the TCA) by backwards propagation. The reference time and position were calculated from the latest TLE set of Cosmos and Iridium as described above. While 13 of the parts show a similar error growth (left part of Table 5), the two remaining objects have a much larger difference (given with their ID in the right part of Table 5). It is probably due to the low perigee of these two objects (~ 400 km) compared to the others (~ 600-800 km). For 13 objects, the first TLEs (upper-left part of Table 5) resulted in a relatively small difference, but the TLEs since then up to 17 days after TCA (middle-left part of Table 5) show extremely fluctuating differences especially in the along-track direction. On the other hand, TLEs which were provided more than 17 days after TCA show consistently growing differences, starting from RTN results shown in the bottom-left part of Table 5. The reason for this fluctuating behaviour might be the length of the data arc used by USSTRATCOM for orbit determination.

Table 5 Comparison of propagated COSMOS-debris TLEs with predicted TCA position

13 cosmos debris	Difference from COSMOS $_{TCA}$			Low perigee	Difference from COSMOS $_{TCA}$		
TCA since TLE epoch [days]	R [km]	T [km]	N [km]	TCA since TLE epoch [days]	R [km]	T [km]	N [km]
-7	0.0 – 0.3	-1.8 – 2.9	0.2 – 0.4	-7 (ID 33767)	0.02	14.30	0.47
-7 ~ -17	-0.5 – 0.4	-23.7 – 45.3	0.0 – 0.6	-7 (ID 33769)	0.10	7.58	0.37
-17	-0.2 – 0.3	-1.8 – 3.4	0.0 – 0.3				

Although the TLE accuracy was analysed using an estimated collision point as the reference, the exact position is unknown also because TLEs near the collision epoch are not sufficiently available. Additionally, the inherent model accuracy and the orbit determination accuracy cannot be estimated in this method. In the following sections, the TLE accuracy is further discussed based on the comparison of TLE orbits with accurate orbit information from locally operated LEO satellites.

4. TLE PRECISION ANALYSIS BASED ON THE PRECISE ORBITS OF GRACE-1 AND TERRASAR-X

In this chapter the accuracy of TLEs is investigated in more detail. Differences between ephemerides generated with USSTRATCOM TLEs and precise orbital ephemerides are presented in section 4.1 and the model differences between the analytical SGP4 and the numerical orbit propagator in section 4.2. The analysis was performed based on the precise orbits of locally operated satellites GRACE-1 and TerraSAR-X (at an altitude of 450 km and 514 km as shown in Table 1). In [1], TLE uncertainties of LEO satellites in the higher altitude are shown using precise orbit data of ERS-1 and ERS-2 spacecrafts, which are operated by the European Space Agency in a mean altitude of 781 km.

The analysis was performed using the well established OD (orbit determination) and OP (orbit prediction) software ODEM (Orbit Determination for Extended Manoeuvres). The OD inside ODEM is formulated as a sequential non-linear least-squares problem based on Givens rotations and the OP is based on a standard numerical integration method for initial value problems. In particular an Adams-Bashforth-Moulton method for numerical integration of ordinary differential equations is adopted. This method employs variable order and step-size and is particularly suited for tasks like the prediction of satellite orbits. The numerical orbit propagator is using a comprehensive model for the acceleration of an Earth orbiting spacecraft under the influence of gravitational and non-gravitational forces, which comprises

- the aspherical gravitational field of the Earth, the Luni-Solar third body gravitational perturbations, the Luni-Solar Earth tides among the mass forces,
- atmospheric drag and solar radiation pressure (SRP) among the surface forces,
- and thrust forces.

The ‘real orbit’ as reference was generated by the software modules POSFIT or RDOD, which are part of the GHOST (GPS High Precision Orbit Determination Software Tool) package developed by GSOC/DLR. POSFIT performs a reduced dynamic orbit determination from a given a priori orbit. It estimates initial conditions, dynamical model parameters and empirical accelerations in a least squares fit. In addition, RDOD uses raw GPS measurements as observations for a precise orbit determination (POD). The position accuracy of the orbits based on POSFIT and POD is better than 2 m and 10 cm, respectively.

4.1 Comparison of USSTRATCOM TLE orbits with precise orbits

The TLE accuracy was assessed by comparing TLE-based orbits with orbits obtained operationally by a POD. Precise orbits of GRACE-1 (Jan.2007-Dec.2008) and TerraSAR-X (since launch, Jun.2007-Mar.2009) were used as reference orbits. POD data of GRACE-1 was taken every 30 seconds; no manoeuvre was performed during the selected period. On the other hand, POD data of TerraSAR-X was taken every 10 seconds including manoeuvres which are performed roughly in a two-week interval.

In the analysis, the bulk of TLE history of the satellites during the considered periods was extracted. Each TLE was propagated to the corresponding POD epoch from -7 (backwards) up to +7 days (forwards) using the SGP4 propagator, and the obtained states were compared with the POD ephemerides.

Table 6 Comparison of TLE propagation with precise orbit (RMS in [km])

GR	*Backwards prop*. [days]							*Forwards prop*. [days]						
	-7	*-6*	*-5*	*-4*	*-3*	*-2*	*-1*	*1*	*2*	*3*	*4*	*5*	*6*	*7*
R	0.391	0.295	0.208	0.135	0.118	0.174	0.258	0.352	0.451	0.545	0.641	0.743	0.836	0.930
T	1.759	1.219	0.827	0.664	0.641	0.762	0.968	1.313	1.813	2.398	3.230	4.384	5.581	6.883
N	0.355	0.355	0.359	0.364	0.368	0.377	0.385	0.390	0.404	0.415	0.426	0.441	0.450	0.461
TX	*Backwards prop*. [days]							*Forwards prop*. [days]						
	-7	*-6*	*-5*	*-4*	*-3*	*-2*	*-1*	*1*	*2*	*3*	*4*	*5*	*6*	*7*
R	0.259	0.226	0.198	0.180	0.171	0.176	0.196	0.228	0.259	0.296	0.337	0.377	0.424	0.468
T	2.644	1.824	1.243	0.906	0.795	0.747	0.796	1.159	1.737	2.266	3.006	4.173	5.235	6.133
N	0.339	0.346	0.357	0.368	0.381	0.397	0.412	0.424	0.444	0.462	0.486	0.508	0.531	0.562

The resulting RMS errors are shown in Table 6 for the RTN components, where the RMS errors of GRACE-1 and TerraSAR-X, which have the similar low altitude (around 500 km), are of comparable sizes in all components.

Results of the backwards propagation show that radial and along-track errors gradually increase from the minimum, which is around 3 days before the TLE epoch. However, the error growth is small within a period about 5 days (ca. 200 m RMS in R, ca. 400 m RMS in N and 800 m RMS in T).

The 7-days forwards propagation shows a comparable error growth for both satellites. The most dominant error exists in the along-track component with a maximum size of about 7 km after 7 days. This error can be caused by a semi-major axis error, by an uncertainty in the ballistic coefficient and also by a prediction error of the solar activity needed for the calculation of the atmospheric density. The larger along-track error of GRACE-1, which has a lower orbit compared to TerraSAR-X, suggests the greater atmospheric influence in the lower orbit. The error in the radial and out-of-plane component results from model difference and orbital parameter evolution (refer to the following section 4.2), where the N component increases slightly and the R component grows by a factor of up to 5 compared to the values of the OD period.

For the TerraSAR-X analysis, manoeuvre influence is to be considered. Only TLEs with an epoch 7 days after and just before the next manoeuvre epoch were extracted from the bulk of TLE history. The RMS error, especially the tangential one of Table 6, increases significantly, when TLEs are included with epochs within 7 days after a manoeuvre date. This suggests that USSTRATCOM TLEs are largely influenced by tracking data up to 7 days before the TLE epoch.

4.2 Comparison of SGP4 propagation with numerical propagation

The orbit data for a space object is in general to be refined regularly in order to enhance the precision of the orbit propagation into the future, which is e.g. important for the calculation of the ground stations contact times and for the provision of antenna pointing information. Adjusting the orbital elements is mainly done by an OD process using measurement data of the current orbit, which can be either tracking data generated by a ground station or GPS navigation solution data generated on board of a satellite.

In order to analyse the differences between the two distinct orbit models, the numerical orbit propagator was used to generate osculating ephemeris data, which served as measurement data for a SGP4 based OD. In other words the mean 2-line elements were determined from a best fit to the generated osculating trajectory.

For satellites operating in LEO, the atmosphere has an important influence on the evolution of an orbit. The atmospheric density itself is directly depending on the solar activity, which can fluctuate dramatically within a few days. To avoid an influence of these fluctuations, the analysis has been performed with constant solar activity parameters.

The analysis was performed in two steps, where at first the mean 2-line elements were determined for fit periods of 1 to 7 days. In the second step the generated TLEs were used to propagate the orbit over up to 7 days. In order to have the same propagation period of 7 days, the end epoch of the fit period was kept constant and consequently the begin epoch of the fit period was different.

4.2.1 SGP4 fitting

Orbit ephemerides were generated for all cases with a step size of 10 seconds both for the SGP4 and for the numerically propagated orbits. Table 7 shows the root mean square (RMS) error of the TLE orbit w.r.t. the numerically propagated orbit in radial, tangential and normal (RTN) directions over the whole fit period. All three error components show a continuous increase with the fit length, where the tangential error is the largest of the three errors and the radial and normal errors are of similar size.

Table 7 RMS error of the fitted TLE orbit w.r.t. the osculating orbit over the fit period

Fit Length [d]	*1*	*2*	*3*	*4*	*5*	*6*	*7*
Tangential [m]	565	624	630	637	647	661	670
Radial [m]	124	129	135	142	150	157	163
Normal [m]	148	146	147	151	156	160	162

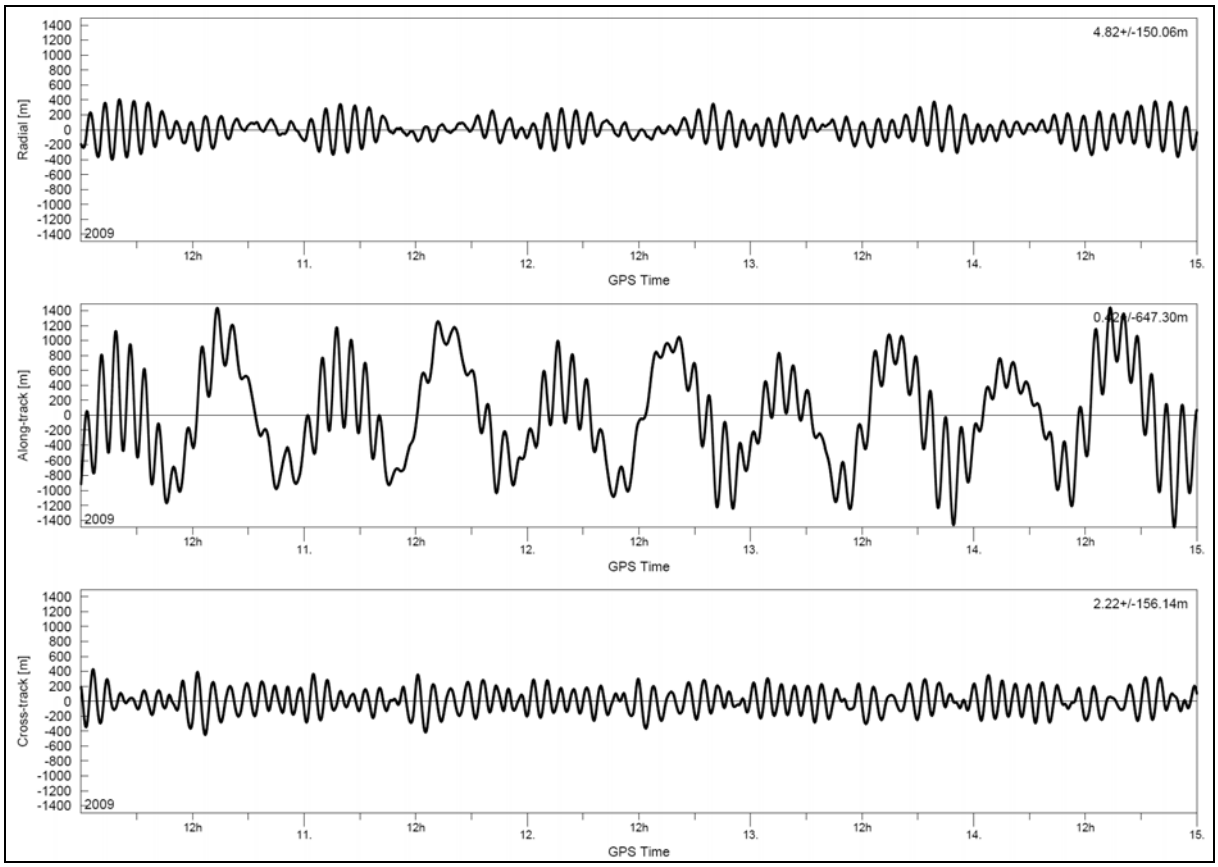

Fig. 1 RTN (radial/tangential/normal) error of a 5-days-TLE-fit w.r.t. numerically propagated orbit

The error pattern looks very similar for each fit period, where a 'long-term-periodic' variation (twice a day) is superimposed by a 'short-term-periodic' (each orbit) one. As an example the RTN errors are plotted in Fig. 1 for a 5-days-TLE-fit, where the maximum error in along-track direction is about 1.5 km.

4.2.2 SGP4 propagation

The statistical evaluation of the propagation period resulted in similar errors for fit-periods between 2 and 7 days as shown in the upper part of Table 8. The increase of the tangential and radial error can be explained by differences in the estimated semi-major axes and ballistic coefficients, whereas the increase of the normal error can be explained by a different node drift due to the semi-major axis error.

The propagation based on a 1-day-fit resulted in extremely high errors in the tangential direction. As the analysis was done for a TerraSAR-X-like orbit with a mean altitude of 510 km, the 1-day-fit analysis was repeated for a CHAMP-like orbit with a mean altitude of 330 km. Even in this case the along-track error shows very high values compared to the others, but smaller compared to the TerraSAR-X-like orbit (refer to the middle part of Table 8). The large errors in tangential direction can be explained by a bad estimation of the ballistic coefficient. The estimation of the ballistic coefficient is better for higher influence of the atmosphere, i.e. for lower altitudes or higher solar activity.

To verify these results, the 5-day-fit case was repeated for a high solar activity ($F_{10.7}$ = 260). As shown in the bottom part of Table 8, the first 3 days of prediction show nearly the same error, whereas the following days show the expected behaviour but only with a factor of about 2 at day 7 of the prediction period.

Table 8 Comparison of TLE propagation based on a 1-7 days fit with numerical propagation (RMS in [m], for TerraSAR-X and CHAMP); low solar activity ($F_{10.7}$ = 100)

TSX (2-7d fit)	*1 day*	*2 days*	*3 days*	*4 days*	*5 days*	*6 days*	*7 days*
R	140 - 220	160 - 260	210 - 320	270 - 390	300 - 420	330 - 440	370 – 480
T	700 - 930	710 - 1190	880 - 1300	1000 - 1930	1100 - 2640	1330 - 3710	1530 - 4990
N	160 - 190	160 - 200	160 - 220	180 - 240	210 - 280	240 - 310	280 - 360
T [m] (1d fit)	*1 day*	*2 days*	*3 days*	*4 days*	*5 days*	*6 days*	*7 days*
TSX	2700	8700	18100	31200	48300	69200	93800
CMP	600	1200	3300	6700	11500	17300	24200
TSX: T [m] (5d fit)	*1 day*	*2 days*	*3 days*	*4 days*	*5 days*	*6 days*	*7 days*
$F_{10.7}$ = 100	740	757	880	1220	1516	1740	2133
$F_{10.7}$ = 260	762	795	844	1006	1103	1121	1191

Compared to the difference between TLE-based obits and POD as shown in the previous section 4.1 (Table 6), the resulting SGP4 model uncertainties for fitting (Table 7) and propagation (Table 8) period are smaller especially in the along-track direction. This means that the TLEs contain further errors in addition to the model uncertainty. Possible main sources of these remaining errors result from the orbit determination process and the uncertainty of the atmospheric density. The influence of atmosphere was exemplarily shown in the lower part of Table 8. The remaining errors in the along-track component, which are dominant and largely growing, also indicate the influence of atmosphere. However, further analysis is necessary for the detail estimation of the remaining errors.

5. FGAN TRACKING CAMPAIGN ANALYSIS

5.1 The FGAN-FHR TIRA System

The only radar in Germany, capable to observe non-cooperative objects in space, is the Tracking and Imaging Radar (TIRA) system of FGAN–FHR. It is located at about 20 km south of Bonn. A photography of the ring building housing TIRA is shown in Fig. 2.

Fig. 2 The TIRA facility (photomontage)

TIRA consists of three major subsystems:

- *34-m parabolic antenna*, fully computer controlled elevation–over–azimuth pedestal. The antenna driving system of TIRA (240 tons) allows a maximum velocity of 24 deg/s (6 deg/s) and a maximum acceleration of 6 deg/s^2 (1.5deg/s^2) in azimuth (elevation).
- L–band narrowband monopulse *tracking radar* allowing closed–loop target tracking with 1.5 MW, 1 ms pulse length, 30 Hz PRF (Pulse Repetition Frequency), gaining for every pulse target range, range rate, azimuth and elevation angles and complex echo amplitude.
- High range–resolution Ku–band *imaging radar*: single–horn imaging radar (guided by tracking radar) with up to 2100 MHz bandwidth (7 cm range resolution) and up to 1500 Hz PRF.

TIRA is mainly used as an experimental system for supporting the development and test of modern radar techniques for space reconnaissance (see also [2]). Major application areas may be categorised as

- high precision orbit determination (mission support, close encounter predictions, re–entry prediction support,...),
- damage/fragmentation and attitude analysis of satellites,
- target cluster analysis,
- data assessment for air/space target identification and classification,
- observation and analysis of the space debris and meteoroid environment.

The monopulse tracking radar (L–band) is operated at 1.333 GHz. The HF power is generated by two Klystrons of which the output power is combined by use of an adjustable hybrid. The generated HF impulse is fed to a 4–horn monopulse feed via harmonic filters, rectangular waveguides, rotary joints in azimuth and elevation, two power dividers for the four feeds and transmitted as a circular polarised signal. Table 9 summarises some typical L–band radar parameters.

Table 9 Summary of typical TIRA L–band tracking radar parameters

Parameter	typical data
Peak power	1.0 MW
Pulse length	1 ms
Lowest elevation	1.4°
Pulse repetition frequency	30 Hz
Radar frequency	1333 MHz
Bandwidth	250 kHz
Modulation	binary phase shift keying
Power amplifier stage	double Klystron
max. Duty cycle	4%
Receiver noise figure	0.35 dB
Matched filter technique	I/Q correlation
Amplitude dynamic range:	
- within an echo	65 dB
- from echo to echo	120 dB
Single pulse sensitivity:	
min. detectable RCS at 1000 km range	-48 dBsm
corresponding object size	2 cm

5.2 Orbit determination and prediction based on FGAN tracking data as well as GPS navigation solution data

The altitude range of the satellites controlled by GSOC reaches currently from 330 km (CHAMP) over 460 km (GRACE-1) to 514 km (TerraSAR-X). As for all three missions precise orbit information (better than 2 m) based on GPS data is available, a tracking campaign with the FGAN radar and the CHAMP and TerraSAR-X satellites were performed on 2009/05/14 over about 24 hours to analyse the OD precision based on FGAN tracking data. Four passes could be used for CHAMP and five passes for TerraSAR-X (see also the tracking data timelines in Fig. 3 and Fig. 4. It should be noted that the Doppler data indicated in the timeline plot were not used for the orbit determination (OD), even if they were generated by the FGAN radar.

The pattern of ground contacts is typical for near polar orbits and ground station locations like the FGAN one, where up to three subsequent orbits with visibility are followed by at least 9 hours with no visibility. Because of the significant influence of the atmosphere in the estimation of the c_D coefficient, a minimum length of 12 hours for the data arc was used for the OD. Based on the resulting orbital elements an orbit ephemeris was generated over a 1.5 days period beginning at the epoch of the last measurement. With this ephemeris the RMS error w.r.t. a precise orbit based on GPS data could be determined.

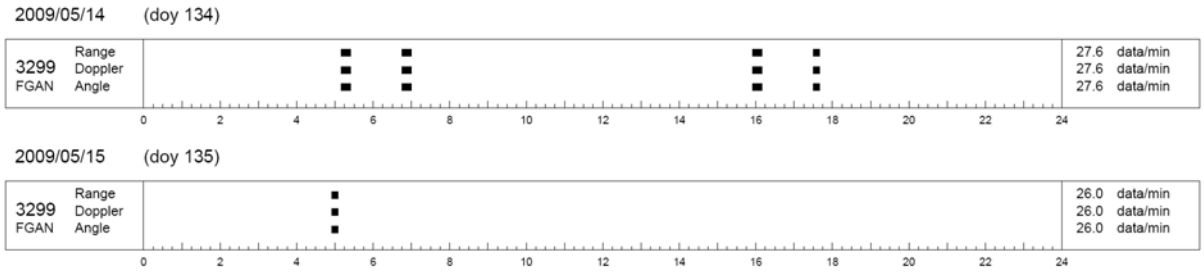

Fig. 3 TerraSAR-X tracking data timeline for FGAN.

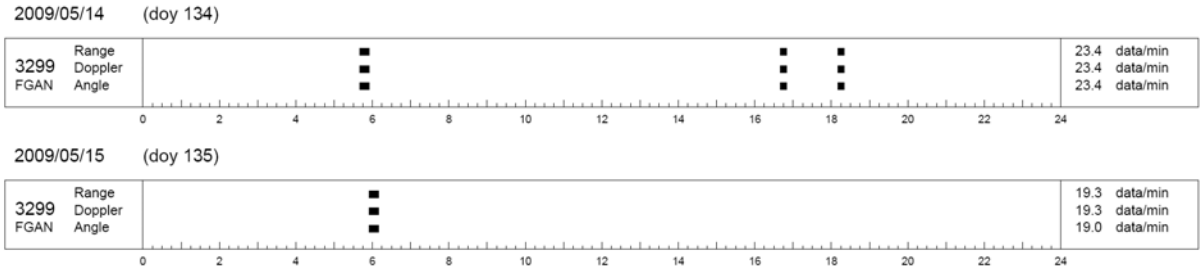

Fig. 4 CHAMP tracking data timeline for FGAN

Four cases were analysed with the collected tracking data under the following conditions:

- Gravity field with an order and degree of 32x32 (nominally used for LEO satellites at GSOC) and 70x70
- Tracking data arcs of 12 h and 24 h

As reference for the FGAN OD accuracy, the same analysis was performed on the basis of GPS navigation solution data as measurements for the same period.

To assess the quality of orbit data received by an OD using FGAN tracking, the two orbit determination results, based on FGAN tracking data and based on GPS navigation solution data, respectively, were propagated over up to 1.5 days after the orbit determination epoch and compared with POD ephemerides. In general the data are comparable, in some cases a factor 2 or 2.5 is seen (refer also to Table 10 and Table 11). Using a higher degree and order of the gravity field leads to better results. In addition, the results listed in Table 10 and Table 11 distinctly shows that orbit prediction is less accurate in a very low orbit like the CHAMP one. The errors can be up to a factor of 20 higher compared to the TerraSAR-X orbit.

Table 10 Tangential RMS (in [m]) of 1.5 days orbit prediction

CHAMP	32x32 gravity field			70x70 gravity field		
	0.5 d	*1.0 d*	*1.5 d*	*0.5 d*	*1.0 d*	*1.5 d*
FGAN (12h OD)	467	1840	4150	366	1307	2686
FGAN (24h OD)	388	1514	3409	303	1050	2104
GPS (12h OD)	307	1196	2680	200	662	1220
GPS (24h OD)	425	1593	3534	344	1157	2297
TerraSAR-X	32x32 gravity field			70x70 gravity field		
	0.5 d	*1.0 d*	*1.5 d*	*0.5 d*	*1.0 d*	*1.5 d*
FGAN (12h OD)	18	83	223	9	40	104
FGAN (24h OD)	70	181	380	53	101	173
GPS (12h OD)	11	45	144	12	49	104
GPS (24h OD)	19	83	224	16	61	132

Table 11 Radial/Normal RMS (in [m]) of 1.5 days orbit prediction

CHAMP	32x32 gravity field		70x70 gravity field	
	radial	*normal*	*radial*	*normal*
FGAN (12h OD)	27	31	16	16
FGAN (24h OD)	22	16	13	3
GPS (12h OD)	18	11	11	6
GPS (24h OD)	23	14	14	3
TerraSAR-X	32x32 gravity field		70x70 gravity field	
	radial	*normal*	*radial*	*normal*
FGAN (12h OD)	4	5	1	1
FGAN (24h OD)	6	7	2	2
GPS (12h OD)	4	6	1	1
GPS (24h OD)	4	5	1	1

The main outcome of this analysis is, that the quality of the OD based on FGAN tracking data is the same order as the reference OD based on GPS navigation solution data. It is also important to mention that this campaign was done during a very low activity phase of the Sun (refer to Fig. 5).

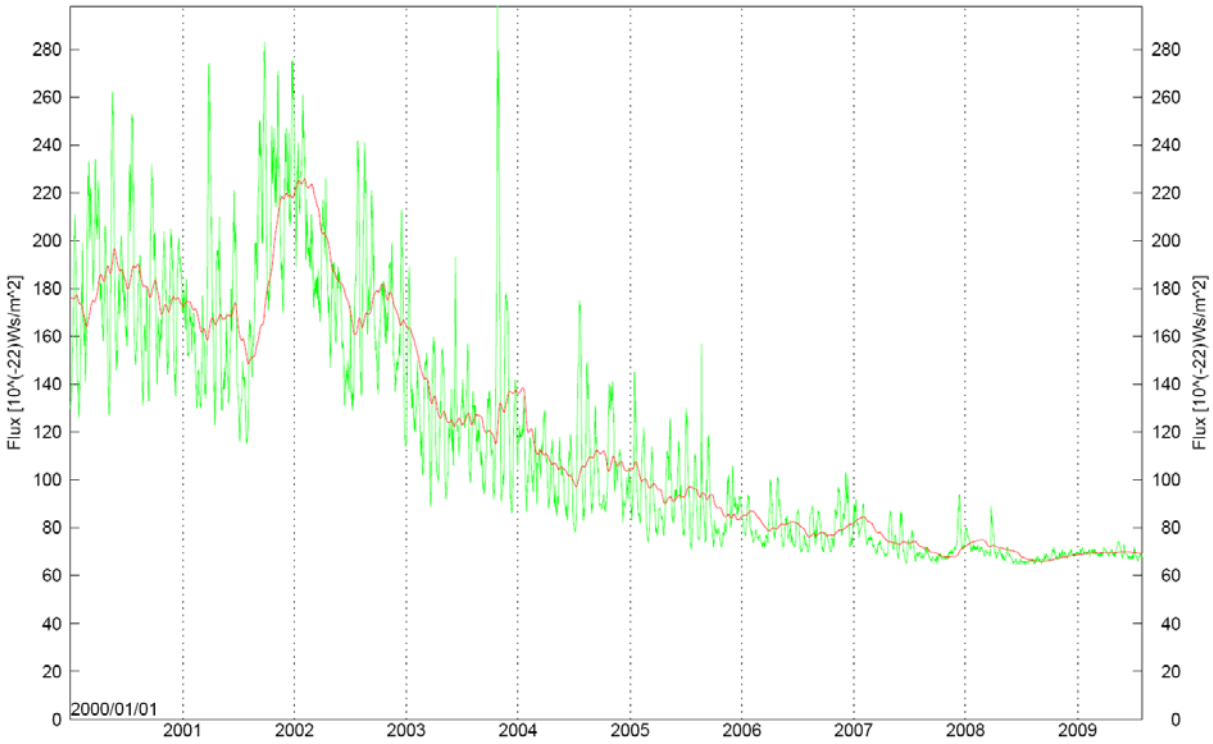

Fig. 5 Daily (green) and 90 days averaged (red) solar activity corresponding to solar flux F10.7 cm line

6. APPLICATION TO COLLISION AVOIDANCE SYSTEM

GSOC is currently implementing a system for collision risk monitoring for LEO satellites operated by the control centre. A prototype software is currently running in an automated process twice a day, which performs a prediction of proximity events for 8 satellites over 7 following days. As shown in the analysis, the radial separation is a good indicator for a critical approach of orbit arcs, because its RMS error is clearly smaller than the RMS in tangential (or along-track) direction. For the 7 days prediction, a threshold of 1 km for radial separation is monitored together with a threshold of 5 km for the distance in order to detect safely critical proximity events.

The obtained TLE RMS errors for each propagation day, shown in Table 6, are used to generate the covariance matrix of space objects in the relevant altitude range. Together with the accurate orbit information of the target spacecraft operated locally at GSOC, the collision probability is then calculated from orbital states and covariance information at the estimated collision epoch.

In case of the high collision risk, it is planned to use FGAN tracking around 1.5 days before the predicted closest approach to refine TLE orbit information. A higher degree and order of gravity field is used for the orbit determination and prediction. The covariance matrix is then also adapted using the RMS errors received in the OD using FGAN tracking (see Table 10 and Table 11).

7. CONCLUSION

For the collision risk management of LEO satellites, proximity statistics and the TLE accuracy as well as the FGAN tracking campaign results were analysed.

The proximity analysis performed over one year shows similar behaviour for TerraSAR-X and GRACE-1. For a typical threshold of < 5.0 km in distance the proximity frequency is double than for a realistic threshold of < 1 km in the radial component.

An analysis of the recent collision event between Cosmos 2251 and Iridium 33 shows that even short-period (~1 day) prediction may result in a large uncertainty of the approach distance, while the critical proximity is detected if the radial separation is considered. Comparing TCA positions by the TLE propagation, the large along-track error and the RMS error growth were shown.

In the TLE precision analysis, SGP4 propagation was compared with POD orbits, and the resulting comparable RMS of GRACE-1 and TerraSAR-X show the increasing error from the minimum, which is around 3 days before the TLE epoch. The differences of the SGP4 model and the model of a numerical orbit propagator were then obtained for OD and OP periods. For the OP, the higher atmospheric influence, which can be either a lower altitude or a higher solar activity, resulted in a better performance of orbit propagation.

The FGAN tracking campaign analysis shows that the OD quality of the FGAN tracking is comparable to that of the GPS navigation solution. In addition, the use of higher degree and order of the gravity field, and also tracking of higher orbits show better results.

These results can be applied to the collision risk management for operational LEO satellites. First, the radial separation (< ~1 km), which has relatively small RMS errors and indicates the possible critical close approach, is also to be monitored in the proximity detection. Additionally, the obtained TLE RMS errors are used for the generation of the covariance matrix for objects in the relevant altitude range. For a better assessment of the collision probability, the orbit determination results of FGAN tracking campaigns can also be used for the update of the covariance information for the tracked object.

The mentioned quality of orbital elements received by an exact orbit determination using FGAN radar data shows that the performance of orbit propagation can be improved by such a process. If a database of orbit data of such a quality would be available instead of the TLE catalogue, the collision avoidance process could be clearly improved and would be more reliable. This demonstrates the need of a new Space Debris Monitoring System as currently planned within the European SSA program.

8. OUTLOOK

The analysis of the TLE fit against osculating orbit ephemerides shows that the solar activity can have an important influence on the prediction accuracy. Further analysis is planned to assess dependency of the RMS propagation error depending on combinations of

- Propagation period,
- Altitude, and
- Solar flux

using precise orbit data of LEO satellites operated at GSOC.

The current prototype monitoring system will be enhanced by analysis tools for a more detailed investigation of proximity events.

9. REFERENCES

[1] J.R. Alarcon-Rodriguez, F.M. Martinez-Fadrique, H. Klinkrad, *Development of a collision assessment tool*, Advances in Space Research 34(2004) 1120-1124

[2] D. Mehrholz, L. Leushacke, W. Flury, R. Jehn, H. Klinkrad, M. Landgraf, *Detecting, Tracking, and Imaging Space Debris*, ESA Bulletin 109 (Feb 2002) 128-134